

Crystal Structure and Magnetic Properties of the New $\text{Zn}_{1.5}\text{Co}_{1.5}\text{B}_7\text{O}_{13}\text{Br}$ Boracite

Roberto Escudero* and Francisco Morales

*Instituto de Investigaciones en Materiales,
Universidad Nacional Autónoma de México. A.
Postal 70-360. México, D.F., 04510 MÉXICO.*

Marco A Leyva Ramirez

*Departamento de Química, Centro de Investigación y
Estudios Avanzados del IPN. 07360, México, D. F.*

Jorge Campa-Molina and S. Ulloa-Godinez

*C. Universitario de Ciencias Exactas e Ingenieras,
Universidad de Guadalajara, Laboratorio de Materiales Avanzados
Departamento de Electronica. 044840, Guadalajara, Jalisco. MÉXICO.*

(Dated: August 29, 2021)

Abstract

New $\text{Zn}_{1.5}\text{Co}_{1.5}\text{B}_7\text{O}_{13}\text{Br}$ boracite crystals were grown by chemical transport reactions in quartz ampoules, at a temperature of 1173 K. The crystal structure was characterized by X-ray diffraction. The crystals present an orthorhombic structure with space group $\text{Pca}2_1$, (No. 29). The determined cell parameters were: $a = 8.5705(3)\text{\AA}$, $b = 8.5629(3)\text{\AA}$, and $c = 12.1198(4)\text{\AA}$, and cell volume, $V = 889.45(5)\text{\AA}^3$ with $Z = 4$. Magnetic properties in single crystals of the new boracite, were determined. The Susceptibility-Temperature ($\chi - T$) behavior at different magnetic intensities was studied. The inverse of the magnetic susceptibility $\chi^{-1}(T)$ shows a Curie-Weiss characteristic with spin $s = 3/2$ and a small orbital contribution, l . At low temperatures, below 10 K, $\chi(T)$ shows irreversibility that is strongly dependent on the applied magnetic field. This boracite is ferrimagnetic up to a maximum temperature of about 16 K, as shows the coercive field. The reduction of the irreversibility by the influence of the magnetic field, may be related to a metamagnetic phase transition.

PACS numbers: Boracites; Ferromagnetism; Metamagnetic transitions; Schottky anomaly; Crystal structure

* escu@servidor.unam.mx

I. INTRODUCTION

The term boracites is at present given to more than 25 isomorphous compounds all with the general formula $\text{Me}_3\text{B}_7\text{O}_{13}\text{X}$, where Me is one of the divalent metals Mg, Cr, Mn, Fe, Co, Ni, Cu, Zn or Cd and X is usually Cl, Br or I. Occasionally X can be OH, S, Se or Te and monovalent lithium substitutes for Me; then the formula becomes $\text{Li}_4\text{B}_7\text{O}_{12}\text{X}$ where X is a halide [1, 2]. Natural and synthetic boracites have attracted the attention of researchers since the early times R. J. Haiÿ [3, 4]. The mineral boracite $\text{Mg}_3\text{B}_7\text{O}_{13}\text{Cl}$, provides the name of this large family [2, 3]. Only other four natural boracites are known: ericaite, chambersite $\text{Mn}_3\text{B}_7\text{O}_{13}\text{Cl}$ [5], congolite $\text{Fe}_3\text{B}_7\text{O}_{13}\text{Cl}$ [6], and trembathite $(\text{Mg,Fe})_3\text{B}_7\text{O}_{13}\text{Cl}$ [6]. Ericaite and trembathite are natural mixed boracites, which have been taken as motivation on this investigation to synthesize other types of mixed boracites. The reason to synthesizing the mixed $(\text{Zn,Co})_3\text{B}_7\text{O}_{13}\text{Br}$ boracites, is related to the idea to understand more about the physical and chemical properties, when combining metals. Boracites have received special attention because of their unusual physical properties [7–10]. In this contribution we present results on the crystallographic characteristics and mainly on the new magnetic properties presented in $\text{Zn}_{1.5}\text{Co}_{1.5}\text{B}_7\text{O}_{13}\text{Br}$. We report the magnetic characteristics from room to low temperatures, investigating the influence of the magnetic field, and the behavior of the specific heat at low temperatures. We found that irreversibility in $\chi(T)$ is strongly dependent on the intensity of the applied magnetic field. We explain this behavior as the transition from low to high spin changes (metamagnetic transition). So, at low field the material behaves as a ferrimagnet, and transits to a ferromagnetic state (high spin) with increasing magnetic intensity. In addition specific heat measurements show a Schottky anomaly at low temperature. We interpreted this anomaly as a resonance between the splitting of spins, from ms states: $3/2$ to $-3/2$, and the thermal energy.

II. EXPERIMENTAL DETAILS

A. Crystal growth

The Schmid method for the sample preparation of crystalline materials was followed [11]. The compound was grown by chemical reaction of vapour phases. Reactants were placed in three fused quartz crucibles of different dimensions separated by small quartz rods, and

vertically aligned. To facilitate the chemical transport, the initial compounds (halogenures, metal oxides, and boric acid) were placed in the bottom, first crucible. The content of this was 1.7 g of B_2O_3 (obtained by dehydrating H_3BO_3); the second crucible contains 0.5 g of ZnO and CoO. Finally, the upper third crucible contains 0.8 g of each divalent metal halides; $CoBr_2$, and $ZnBr_2$. These were placed inside a quartz ampoule under vacuum. The chemical transport reactions were carried out by heating the ampoule in a vertical oven with the following heating steps: 1173 K over a period of 50 hours, and 913 K over a period of 20 hours. At the end of this process, once at room temperature we observed small single crystals boracites. The single crystals of the mixed boracites show an intense purple color and approximately 3 mm in size, those crystals mostly are formed at the end of the lower crucible.

B. Crystal structure analysis

X-ray data were collected using graphite monochromated $MoK\alpha$ radiation $\lambda = 0.71073$ Å in a Enraf-Nonius Kappa-CCD diffractometer. Data reduction was made by the Denzo-Scalepack software [12]. The Structure was solved by direct method and refined by full-matrix least squares, using the SHELX97 package software [13].

C. Refinement details

Refinement of Boracites by single-crystal techniques is complicated because the very frequent twins created in the growing process [14]. In order to solve this complication we used a twin matrix method to refine the crystal structure. We detected two domains in the studied single crystal by using the package PLATON [15]. In order to have a better interpretation of the studied electronic densities a Multi-Scan absorption correction was used with the SADABS software [13]. Due to high electron density of the Bromine atoms, the localization of light elements becomes complicate, and also the corresponding refinement: This fact explains the low isotropic temperature factor(U_{iso}) in the Boron and Oxygen atoms. Accordingly, the X-ray pattern of the studied sample was refined isotropically. In this case was necessary to consider a restrain for the occupation. This was taken as 0.5 of Zn/Co atoms; with this restrain we obtained good agreement for the anisotropical values

for Zn and Co atoms. thus, good convergence and low R value were obtained.

D. Magnetic measurements

Magnetic measurements were performed using a MPMS magnetometer (Quantum Design). $M - T$ measurements were obtained at three different magnetic intensities; 100, 1000, and 5000 Oe. The data acquisition modes were the standard Zero Field Cooling (ZFC) and Field Cooling (FC). After these measurements we obtained the magnetic susceptibility as a function of the temperature $\chi(T)$ in terms of cm^3/mol , and the Pascal constant were added. In addition, we performed isothermal magnetization measurements cycles at various temperatures.

E. Specific heat measurements

Specific heat measurements C_P as a function of temperature were performed using a thermal relaxation method, utilizing a PPMS (Quantum Design) apparatus. Measurements were performed at low temperatures with applied magnetic field of 0, 100 and 5000 Oe. The C_P values were corrected subtracting the addenda due to the sample support and the grease used to glue the sample on the support.

III. RESULTS AND DISCUSSION

A. Structural characterization

X-ray diffraction analysis reveals that $\text{Zn}_{1.5}\text{Co}_{1.5}\text{B}_7\text{O}_{13}\text{Br}$ compound crystallizes in an orthorhombic structure with space group $\text{Pca}2_1$ (No. 29). The structural parameters determined are summarized in I. In Supplementary Material the final refined positional and thermal parameters are given in Table 2, and the main interatomic distances and angles are given in Table 3. The unit cell for this boracite is shown in 1.

The bond distances and angle values on first approach, looks abnormal. The reason is because the difference between the coordination polyhedral bond distance is too big. For instance, the octahedral polyhedral whose central atoms are Br, is coordinated with six Zn or Co atoms; the average bond distances Zn(1)-Br and Co(1)-Br are 2.576(4) and

TABLE I. Crystal data and data parameters of $\text{Zn}_{1.5}\text{Co}_{1.5}\text{B}_7\text{O}_{13}\text{Br}$ boracite.

Compound	Boracite
Chemical formula	$\text{Co}_{1.5}\text{Zn}_{1.5}\text{B}_7\text{O}_{13}\text{Br}$
Formula weight	550.03
Cryst size [mm]	0.075 x 0.11 x 0.19
Cryst. system	Orthorhombic
Space group	$\text{Pca}2_1$
a , [Å]	8.5705(3)
b , [Å]	8.5629(3)
c , [Å]	12.1198(4)
V , [Å ³]	889.45(5)
Z	4
$\rho(\text{calc.})$, [Mg/m ³]	4.107
μ [mm ⁻¹]	11.366
$F(000)$	1038
Index range	$-9 \leq h \leq 10$ $-11 \leq k \leq 11$ $-15 \leq l \leq 13$
2θ [°]	54.80
Temp, [K]	293(2)
Refl. collected	10425
Refl. unique	2027
Refl. observed (4σ)	1273
R (int.)	0.0601
No. variables	116
W. scheme x/y	$w^{-1} = \sigma^2 F_0^2 + (xP)^2 + yP$ $P = (F_0^2 + 2F_C^2)/3$
GOF	1.001
Final R (4σ)	0.0334
Final wR2	0.0708
Larg. res. peak [e/Å ³]	3.140

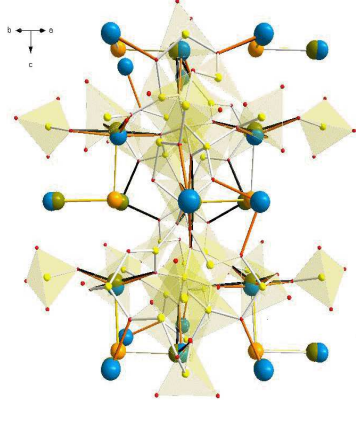


FIG. 1. (Color online) This figure displays the Unit cell for $\text{Zn}_{1.5}\text{Co}_{1.5}\text{B}_7\text{O}_{13}\text{Br}$ boracite. Atoms are marked in different colors and descending in size, as: blue balls, Zn; green balls, Co; orange, Br; yellow, B; and small red ones, Oxygens.

2.756(5) Å, which implies a big distortion of the polyhedrons. This polyhedral distortion is a characteristic of every boracite compound [16–20]. We found that the diagonal value between the lattice constant a and b is 12.1151 Å, which is almost the same value of the c parameter (12.1198 Å). Likewise, observing the bond distance between different tetrahedra, as BO_4 , we clearly can distinguish very strong deformations. These deformations may provokes that the total atom charge in the crystal structure not be neutralized, and consequently zones with negative and positive charge could appear. This distortion generates electric dipoles along the preferred direction of the crystal structure.

B. Magnetic behavior

2 displays the susceptibility as a function of temperature measured at 100 Oe. At first glance we can see two characteristics: In FC mode $\chi(T)$ presents a paramagnetic behavior at high temperature, the values are quite small and close to zero. At low temperature, about 50 K the χ value gradually increases and at about 12 K χ presents a rapid increase; at 2 K has a huge value of about $4 \text{ cm}^3/\text{mol}$. However, in the ZFC mode at 2 K also, χ is negative but rapidly grows as the temperature rises, the a maximum values at 11 K is about $0.23 \text{ cm}^3/\text{mol}$. This is small in comparison to the maximum value in FC mode. A that maximum the two modes present an irreversible behavior when the temperature decreases. This behavior clearly is displayed in the insert of 2. 3 shows the inverse susceptibility $\chi^{-1}(T)$,

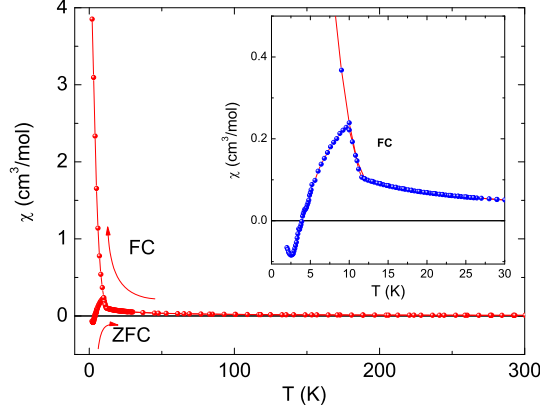


FIG. 2. (Color online) Magnetic susceptibility vs. Temperature, $\chi(T)$ of $(\text{Zn,Co})_3\text{B}_7\text{O}_{13}\text{Br}$ borate single crystal measured with 100 Oe, in ZFC and FC modes, the arrows show the increasing/decreasing of the temperature. At low temperature the irreversibility is clearly observed. The insert displays the rapid increase of the susceptibility in the FC mode, occurring at about 12 K.

used to determine the magnetic characteristics. As already mentioned, at high temperature the compound follows a Curie-Weiss law that was fitted with a constant, $C = 2.46 \pm 0.03 \text{ cm}^3\text{K/mol}$, and an extrapolated Curie-Weiss temperature θ_{CW} from -19 to -24 K. This C value is well fitted with a total number of Co spins contribution $s = 3/2$, and a small orbital angular contribution $l < 1$. It is important to mention that in orthorhombic crystals (also in cubic crystals) structures the orbital moment vanishes at first order. In this case the small deformation of the orthorhombic structure (the angles are not exactly 90 degrees) gives the possibility, as we observed, that the orbital angular moment l is not totally quenched. In the top insert of this figure we plotted an amplification of the inverse susceptibility from 2 K to 20 K. At about 12.7 K an abrupt change of slope occurs. In the inferior insert we display the effective number of Bohr magnetons, μ_B , at room temperature are equal to $4.3 \mu_B$. In the same figure and at low temperature a ferrimagnetic transition can be deduced; this ferrimagnetic ordering is according to the negative θ_{CW} values obtained by the fitting. nevertheless, as a confirmation of the ferrimagnetic behavior, and the crossover to high spin by influence of the magnetic intensity, we studied the isothermal magnetic $M - H$ characteristics at different temperatures, from 2 K to 20 K. The coercive field already is observed, and it is shown in the main panel of 4. It is clear that the coercive field tends to disappear at temperatures of the order of 15 K. The insert in this figure also presents one

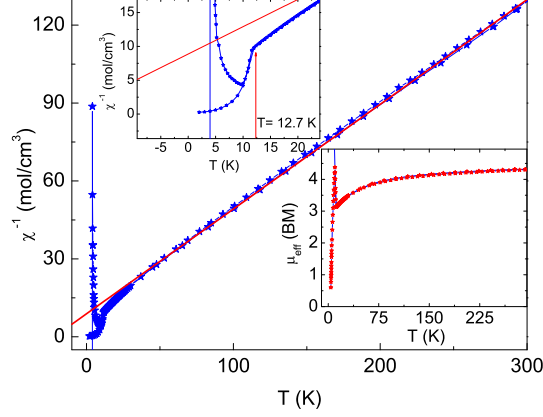


FIG. 3. (Color online) Inverse of the magnetic susceptibility $\chi^{-1}(T)$ measured in ZFC and FC modes, at 100 Oe. The continuous line in the main panel and the top insert shows the fit to the Curie-Weiss law. Curie constant value was determined to be $C = 2.46 \pm 0.03 \text{ cm}^3 \text{ K/mol}$, and θ_{CW} changes from 19 - 24 K. The top insert shows an amplification of the main panel at low temperature. There, the vertical arrow marks the change of the slope, which is about 12.1 K. The inferior insert displays the effective number of Bohr magnetons, determined as $4.25 \mu_B$ at room temperature.

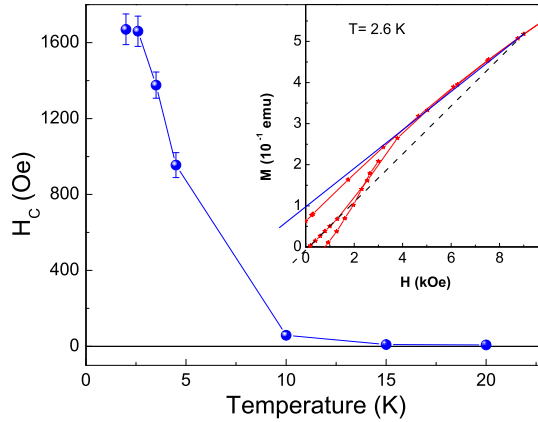


FIG. 4. (Color online) Coercive field determined by isothermal $M - H$ measurements at different temperatures. The ferromagnetic ordering persists only around 15 - 20 K. The insert shows the influence of magnetic field in the magnetic properties, This small spin crossover indicates a metamagnetic transition changing the magnetic ordering from ferrimagnetic to ferromagnetic.

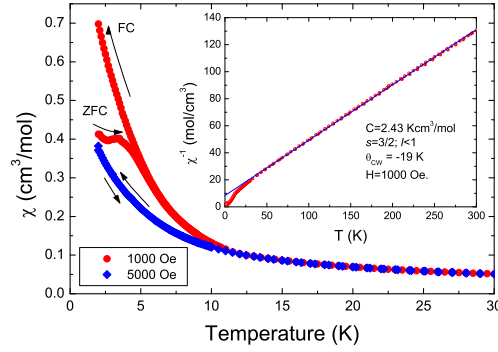


FIG. 5. (Color online) Main panel presents the magnetic susceptibility, $\chi(T)$, measured with 1000 Oe, from 30 K to 2 K. The characteristic shows important differences of behavior that are strongly dependent on the intensity of the magnetic field applied. At higher field, 5000 Oe, the behavior is completely reversible, as noted by completed reversibility. This behavior marks the metamagnetic transition, by influence of the applied magnetic field.

isothermal $M - H$ at 2.6 K to illustrate crossover from low spin to high spin.

5 displays the susceptibility as a function of temperature measurements into magnetic fields of 1000 Oe and 5000 Oe. Note that the irreversible temperature changes at lower temperature and disappears at 5000 Oe. We interpreted this behavior as a metamagnetic transition. However in order to have a clear confirmation of this feature we plotted at low temperature isothermal $M - H$ measurements. This characteristic shows a small but discernible change from low to high spin as the magnetic intensity is increased. Metamagnetism is due to the applied field strength that overcome the crystal anisotropic force, producing an abrupt change in the internal order [21].

C. Specific heat

Lastly, in order to confirm the complicated physical characteristics of this boracite, we studied the specific heat at low temperatures. Our experiments show an anomalous wide peak, that we characterized as a Schottky anomaly (6). This occurs at low temperatures, where spin population may be excited by thermal energy between e_g and t_{2g} levels of the system. This Schottky anomaly occurs at about 4.3 K, the thermal energy at this temperature is about 370×10^{-6} eV, corresponding approximately to the splitting of the $\pm s = 3/2$

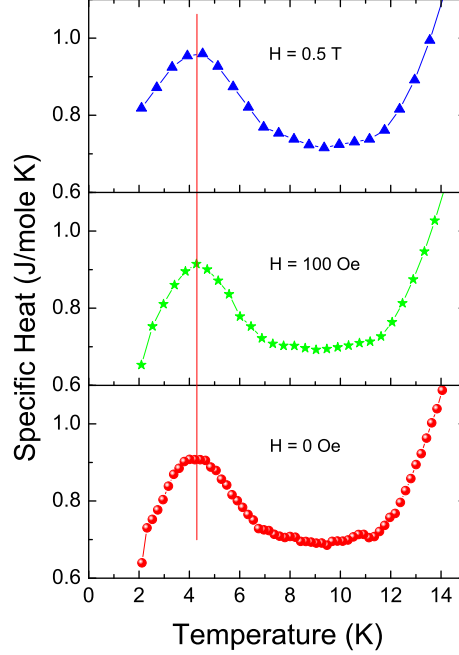


FIG. 6. (Color online) Specific heat at low temperature of the boracite $\text{Zn}_{1.5}\text{Co}_{1.5}\text{B}_7\text{O}_{13}\text{Br}$ measured at magnetic field intensities of 0, 100, and 5000 Oe. The feature displayed at about 4.5 K, clearly can be catalogued as a Schottky anomaly.

states.

IV. CONCLUSIONS

A new $\text{Zn}_{1.5}\text{Co}_{1.5}\text{B}_7\text{O}_{13}\text{Br}$ boracite was synthesized by the vapor transport method. The compound has a orthorhombic crystal structure, with small distortions, and with the space group $\text{Pca}2_1$ (No. 29) and cell parameters $a = 8.5705(3)$, $b = 8.5629(3)$, and $c = 12.1198(4)$ Å, and Volume = $889.45(3)$ Å³. Magnetic measurements performed as a function of temperature and at different magnetic intensities show that the general behavior at low temperature changes; first at all, the irreversibility disappears at an intensity of about 5000 Oe, and the anomalies change. This behavior is because the low to high spins crossover, affecting the general characteristics. We identify this reduction of irreversibility as a metamagnetic transition. Lastly, specific heat measurements at low temperature show an anomaly that clearly was identified as a Schottky anomaly.

ACKNOWLEDGMENTS

RE thanks CONACyT project 129293, and DGAPA UNAM project IN100711. FM thanks the partial support of DGAPA UNAM project IN111511. We also thank to R. Reyes and to F. Silvar for help in technical problems.

-
- [1] Levasseur, A. *Sur de nouveveaux borates ages dinsertion*. PhD thesis, Universit de Bordeaux I, France, No. d'order (1979) 409, 1-5.
 - [2] Nelmes, R. J. *J. Phys. C: Solid State Phys.*, **1974**, 7, 3840-3853.
 - [3] Dana, J. D. *Dana's System of Mineralogy*, C. Palache, H. Berman. and C. Frondel, Edited John Wiley Press, New York, 1951.
 - [4] Hankel, W. G. *Ueber die Thermoelektrischen Eigenschaften des Boracites. Abhandlungen der Matematisch-Physischen Classe. Der Koeniglich Saechsischen. Gesellschaft der Wissenschaften*, Vol. 4. S. Hirtzel, Leipzig, 1859.
 - [5] Honea, R. M. & Beck, F. R. *Am. Mineralogist*, **1962**, 47, 665-671.
 - [6] Dana, J. D. *New Mineralogy*, 8th edn (ed. by R. V. Gaines, H. Catherine, W. Skinner, E. E. Foord, B. Mason and A. Rosenzweig), pp. 25.5-25.6. John Wiley Inc. New York, 1997.
 - [7] Smart L. and Moore, E. *Solid State Chemistry, An Introduction*, edited London: Chapman and Hall, 1992.
 - [8] Mathews, S.; Ramesh, R.; Venkatesan T.; J. Benedetto, *Science*, **1997**, 276, 238-240.
 - [9] Castellanos-Guzman, A. G.; Campa-Molina, J.; Reyes-Gomez, J. *Journal of Microscopy*, **1997**, 185, 1-8.
 - [10] Campa-Molina, J.; Castellanos-Guzman, A. G. *Solid State Commun.*, **1994**, 89, 963-969.
 - [11] Schmid, H. *J. Phys. Chem. Solids*, **1965**, 26, 973-988.
 - [12] Otwinowski, Z.; Minor, W. *Processing of X-ray Diffraction Data Collected in Oscillation Mode*, Vol. 276: Macromolecular Crystallography, part A, p.307-326, C.W. Carter, Jr.
 - [13] Sheldrick, G. M. *Acta Cryst.*, **2008**, A64, 112-122.
 - [14] Abrahams, S. C.; Bernstein, J. L.; Svensson, C. *J. Chem. Phys.*, **1981**, 75, 1912-1918.
 - [15] Spek, A. L. *Acta Cryst.*, **1990**, A46, C34.
 - [16] Ascher, E.; Schmid, H.; Tar, D. *Solid State Commun.*, **1964**, 2, 45-49.

- [17] Ascher, E.; Rieder, H.; Schmid, H.; Stössel, H *J. Appl. Phys.*, **1966**, 37, 1404-1405.
- [18] Thompson, P.; Cox, D. E.; Hastings, J. B. *J. Appl. Cryst.*, **1987**, 20, 79-83.
- [19] Kubel, F.; Mao, S. Y.; Schmid, H *Acta Cryst. C*, **1992**, 48, 1167-1170.
- [20] Ito, T.; Morimoto, N.; Sadanaga, R. *Acta Cryst.*, **1951**, 4, 310-316.
- [21] Hurd, C. M. *Contemp. Phys.*, **1982**, 23, 469-493.